Carolyn M. Bogan for the initial suggestion concerning the computational method.

References and Notes

(1) G. C. Berry and E. F. Casassa, *J. Polym. Sci., Part D*, 4, 1 (1970); E. F. Casassa, *J. Polym. Sci., Part A-2*, 8, 1651 (1970).
(2) F. Candau, P. Rempp, and H. Benoit, *Macromolecules*, 5, 627 (1972).
(3) D. Decker, *Makromol. Chem.*, **125**, 136 (1969); I. Noda, T. Horikawa, T. Kato, T. Fujimoto, and M. Nagasawa, *Macromolecules*, 3, 795 (1970); J.-C. Meunier and R. van Leemput, *Makromol. Chem.*, **147**, 191 (1971); J. Pannell, *Polymer*, **12**, 558 (1971); G. C. Berry, *J. Polym. Sci., Part A-2*, 9, 687 (1971); F. Candau and P. Rempp, *Eur. Polym. J.*, 8, 737 (1972); J.-G. Zilliox, *Makromol. Chem.*, **156**, 121 (1972).
(4) D. J. Bauer and L. J. Fetters, *Rubber Chem. Technol.*, 51, 406 (1978).
(5) T. Altares, D. P. Wyman, V. R. Allen, and K. Meyersen, *J. Polym. Sci., Part A-2*, 3, 4131 (1965).
(6) J. Roovers, *Polymer*, **20**, 843 (1979). See also references therein.
(7) T. A. Orofino, *Polymer*, **2**, 305 (1961); G. C. Berry, V. C. Long, and L. M. Hobbs, *ibid.*, **5**, 31 (1964); E. F. Casassa, *J. Chem. Phys.*, **41**, 3217 (1964); E. F. Casassa, *ibid.*, **45**, 2811 (1966); M. Kurata and M. Fukatsu, *ibid.*, **41**, 2934 (1964).
(8) G. C. Berry and T. A. Orofino, *J. Chem. Phys.*, **40**, 1614 (1964).
(9) E. F. Casassa and G. C. Berry, *J. Polym. Sci., Part A-2*, 4, 881 (1966).
(10) E. F. Casassa and Y. Tagami, *J. Polym. Sci., Part A-2*, 6, 63 (1968).
(11) G. C. Berry, *J. Polym. Sci., Part A-2*, 6, 63 (1968).
(12) H. Yamakawa, "Modern Theory of Polymer Solutions", Harper and Row, New York, 1971, Chapter 3.
(13) M. Fixman, *J. Chem. Phys.*, **23**, 1656 (1955).
(14) We have modified the categories of Berry and Orofino in two ways: our group 0 is part of their group 1, and the first three Γ_1 terms in our group 2 (eq 12) correspond to terms in their group 1. It seems to us that our choice in the latter instance is logically preferable.
(15) This tabulation should be compared with Table I in ref 8 for regular combs. Apart from the differences in cataloging noted above, the symmetry of the regular comb renders pairs of diagrams that appear in our scheme identical. Table I in ref 8 also has errors, which have been corrected here, in the group 2 enumeration. The Berry–Orofino chain parameters y and y/r translate to n_b and $n_0/(f+1)$ in this paper.
(16) It is obviously artificial to identify a statistical backbone segment with just one chemical unit affording a locus for attachment of a branch. However, if $\bar{f}$ is far less than n_0, this simplification has no sensible effect on the distribution of branches in the system.
(17) H. Cramér, "Mathematical Methods of Statistics", Princeton University Press, Princeton, 1946, pp 175 and 195.

Asymmetry of Flexible Chains, Macrocycles, and Stars

Wayne L. Mattice

Department of Chemistry, Louisiana State University, Baton Rouge, Louisiana 70803.
Received October 16, 1979

ABSTRACT: Instantaneous asymmetry of the distribution of chain segments has been characterized for four types (linear chain, macrocycle, three-star, four-star) of flexible unperturbed polymers containing fixed bond angles. Stars contain the same number of atoms in each branch. Results for large polymers are in harmony with those reported by several previous investigators. Asymmetry of large polymers increases in the order four-star < macrocycle < three-star < linear chain. Development of the limiting asymmetry is characterized in each case. Individual principal components of the mean square radius for the four types of molecules considered reflect differences in both asymmetry and characteristic ratio. Almost all differences in mean square radius of gyration for these molecules can be attributed to variation in the averaged largest principal component of the mean square radius when the number of bonds is large. Thus cyclization of a long linear chain demands a major reduction in the largest principal component but only minor adjustment of the remaining principal components.

The squared radius of gyration, s^2, characterizes the extension of chain atoms about their center of mass for a specified configuration of a polymer molecule. Asymmetry of this spatial distribution can be assessed through evaluation of the principal components, $L_1^2 \geq L_2^2 \geq L_3^2$, $s^2 = L_1^2 + L_2^2 + L_3^2$. Interest is focused on departures from unity of any two independent ratios, such as L_2^2/L_1^2 and L_3^2/L_1^2.

If the polymer molecule is flexible, average extension of atoms about the center of mass is characterized in a straightforward manner by the mean square radius of gyration, $\langle s^2 \rangle$. Asymmetry of the spatial distribution, however, is subject to different definitions which yield contrasting results. The starting point in each case can be viewed as the radius of gyration tensor, $\mathbf{S}_{x2}$, for every accessible configuration, with every $\mathbf{S}_{x2}$ expressed in an internal coordinate system rigidly attached to a specified part of the molecule. This coordinate system might, for example, be defined by the orientation of two consecutive bonds.[1] One definition of asymmetry utilizes the principal components ($\langle S_{2,a} \rangle \geq \langle S_{2,b} \rangle \geq \langle S_{2,c} \rangle$, $\langle s^2 \rangle = \langle S_{2,a} \rangle + \langle S_{2,b} \rangle + \langle S_{2,c} \rangle$) of $\langle \mathbf{S}_{x2} \rangle$, where $\langle \mathbf{S}_{x2} \rangle$ denotes the average of all accessible $\mathbf{S}_{x2}$, averaging being accomplished in the internal coordinate system.[1] If this definition of asymmetry is employed, all flexible homopolymers of sufficiently high molecular weight will be found to possess spherical symmetry ($\langle S_{2,a} \rangle = \langle S_{2,b} \rangle = \langle S_{2,c} \rangle$).[1-3] Smaller polymers will not have a spherically symmetric spatial distribution. In such cases asymmetry may depend upon the precise location of the internal coordinate system in which the $\mathbf{S}_{x2}$ are expressed.[2,3]

An alternative definition of asymmetry, and the one to be employed in the remainder of this work, focuses attention on the average, $\langle L_i^2 \rangle$, $i = 1, 2, 3$, of the corresponding principal moments for all accessible $\mathbf{S}_{x2}$. This definition thus permits an assessment of the average instantaneous asymmetry of the spatial distribution. Large flexible polymer chains are definitely asymmetric when this definition,[4-6] or one based on the end-to-end vector,[7] is adopted. Furthermore, sufficiently large unperturbed flexible chain molecules have been found to all have virtually identical asymmetries, as measured by $\langle L_2^2 \rangle / \langle L_1^2 \rangle$ and $\langle L_3^2 \rangle / \langle L_1^2 \rangle$. Validity of this assertion is illustrated by results collected in Table I. Monte-Carlo calculations have been carried out for chains on a cubic lattice[4-6] as well as for rotational isomeric state models for unperturbed poly(methylene),[1] poly(oxyethylene),[8] and poly(thiaethylene).[9] Averages of these results are $\langle L_2^2 \rangle / \langle L_1^2 \rangle =$

0024-9297/80/2213-0506$01.00/0

Table I
Ratios of Averaged Principal Components of the Mean Square Radius for Unperturbed Flexible Linear Chains

model	no. of bonds	$\langle L_2^2\rangle/\langle L_1^2\rangle$	$\langle L_3^2\rangle/\langle L_1^2\rangle$	ref
Monte-Carlo				
cubic lattice	50	0.229	0.085	4
cubic lattice	62	0.231	0.085	6
cubic lattice, 6-choice walk	100	0.223	0.086	5
cubic lattice, 5-choice walk	200	0.224	0.082	5
poly(methylene)	∞	0.225	0.083	1
poly(oxyethylene)	∞	0.23	0.076	8
poly(thiaethylene)	∞	0.22	0.077	9
analytical				
spring bead model	∞	0.246	0.108	10, 11

Table II
Asymmetry for Large Flexible Unperturbed Macrocycles and Stars

	$\langle L_2^2\rangle/\langle L_1^2\rangle$		$\langle L_3^2\rangle/\langle L_1^2\rangle$	
molecule	cubic lattice[a]	present work	cubic lattice[a]	present work
three-star	0.334	0.326	0.118	0.116
macrocycle	0.362	0.37	0.154	0.155
four-star	0.412	0.39	0.161	0.153

[a] Reference 12.

0.226 and $\langle L_3^2\rangle/\langle L_1^2\rangle = 0.082$. An approximate analytical approach based on a spring bead model yields somewhat higher values for these ratios, corresponding to a less asymmetric spatial distribution.[10,11]

Large macrocycles on a cubic lattic also have a characteristic asymmetry.[12] While rotational isomeric state treatments of poly(oxyethylene) and poly(thiaethylene) yield markedly different macrocyclization equilibrium constants, large macrocycles once formed have essentially identical asymmetries[8,9] which are in good agreement with those found for macrocycles on a cubic lattice. Macrocycles, as expected, are found to be much less asymmetric than large unperturbed flexible acyclic chains. A similar situation is obtained for sufficiently large unperturbed flexible three-stars and four-stars, molecules with three (or four) chains of identical contour length emanating from a common atom.[12] Asymmetries increase in the order four-star < macrocycle < three-star < linear chain if the molecule contains a sufficiently large number of atoms[12] (Tables I and II).

Calculations are reported here as a function of the number of chain atoms for linear chains, macrocycles, three-stars, and four-stars with fixed bond angles in the range 80–120°. Attention is given to the manner in which small polymers of all four types approach the asymmetry characteristic of extremely large polymers. Changes in individual $\langle L_i^2\rangle$ are also assessed.

Calculations

Each molecule contains n identical atoms connected by $n - 1$ identical bonds (n bonds for macrocycles). Long-range intramolecular interactions are assumed to be completely compensated by polymer–solvent interactions. Stars always have the same number of bonds in each branch. Tetrafunctional branch points have tetrahedral geometry. All other bond angles are held constant at 120, 110, 100, 90, or 80° (supplements θ = 60, 70, 80, 90, 100°). Internal bonds have three rotational states, t and $g^{\pm}$, which are equally probable and independent of rotational states occupied by neighboring bonds. Dihedral angles for t and $g^{\pm}$ states are 0 and ±120° for all internal bonds except those involving the atom at a trifunctional branch point. If a trifunctional branch point occurs at C^{γ}, rotational states for bond C^{β}–C^{γ} are assigned where there is a trans orientaton for C^{α}–C^{β}–C^{γ}–C^{δ_1} and a trans orientation for C^{α}–C^{β}–C^{γ}–C^{δ_2}. If the dihedral angles for these two states are $\pm\varphi$ ($\varphi < 90°$), the remaining rotational state has φ = 180°. Results become independent of bond angle and rotational state location at the branch point as n approaches infinity.

Monte-Carlo methods were used to grow $4N$ molecules, N in each of four sets, with specified n, θ, and molecular architecture. The L_i^2 and s^2 were averaged for molecules in each of the four sets. Reported standard deviations are those obtained from averages for the four sets. The value of N was 15 000 for linear chains and three-stars and 250(n − 13) for four-stars. Chains satisfying criteria for macrocycle formation were selected from four sets containing 15 000 linear molecules each. Nine different groups were temporarily selected with the use of all combinations of i, j in the criteria $r^2_{\text{"macrocycle"}}/\langle r^2\rangle_{\text{acyclic}} < a_i$ and $\Delta\theta < b_j$. Here $\langle r^2\rangle_{\text{acyclic}}$ is the mean square unperturbed end-to-end distance for the linear chains, $\Delta\theta$ is the absolute value of the displacement of the bond angle formed on cyclization from the value found for all other bonds in the chain, the a_i are 0.05, 0.10, and 0.20, and the b_j are 15, 30, and 60°. The final group was selected from the nine temporary groups by choosing the one containing at least 100 cyclic chains and having the smallest value of $j + 3i$. Chains called "macrocycles" are thus acyclic chains with an extremely small end-to-end distance. Values of $\langle r^2\rangle_{\text{"macrocycle"}}/\langle r^2\rangle_{\text{acyclic}}$ were 0.03 for the largest chains studied.

Results and Discussion

Linear Chains. Behavior of linear chains as n tends toward infinity can be predicted from the Monte-Carlo results collected in Table I. Since properties of cyclic chains, to be discussed below, will be evaluated from an appropriately selected subset of acyclic chains, it is important to establish the validity of the set of linear chains. Figures 1–3 achieve this objective. They will also demonstrate the manner in which the limiting asymmetry is developed.

Figure 1 depicts the characteristic ratio, $\langle s^2\rangle/nl^2$, for linear chains of indicated n and θ. (The characteristic ratio is defined here as $\langle s^2\rangle/nl^2$, rather than $\langle r^2\rangle/nl^2$, because $\langle r^2\rangle$ is zero for macrocycles and ambiguous for stars.) In each case t and $g^{\pm}$ states are equally weighted and independent of rotational states adopted at neighboring bonds. The characteristic ratio becomes a linear function of n^{-1} when a sufficient number of bonds is present. Straight lines are drawn so that the intercept has the value given by[13]

$$[\langle s^2\rangle/nl]_{\infty} = (1/6)(1 + \cos\theta)(1 - \cos\theta)^{-1} \quad (1)$$

Chains actually studied attain the asymptotic limit only when θ is 90°. The expected intercept is a reasonable extrapolation of data in the remaining four cases. The straight lines in Figure 1 have the expected slope,[13] when allowance is made for n in ref 13 to be the number of bonds, while here n is the number of atoms.

Ratios of averaged principal moments are depicted in Figures 2 and 3. All but two of the straight lines are given by eq 2 or 3 (θ is in degrees).

$$\langle L_2^2\rangle/\langle L_1^2\rangle = 0.225 + (-2.18 + 0.0272\theta)n^{-1} \quad (2)$$

$$\langle L_3^2\rangle/\langle L_1^2\rangle = 0.082 + (-2.18 + 0.0277\theta)n^{-1} \quad (3)$$

Lines for θ = 70° in Figure 2 and θ = 100° in Figure 3 have

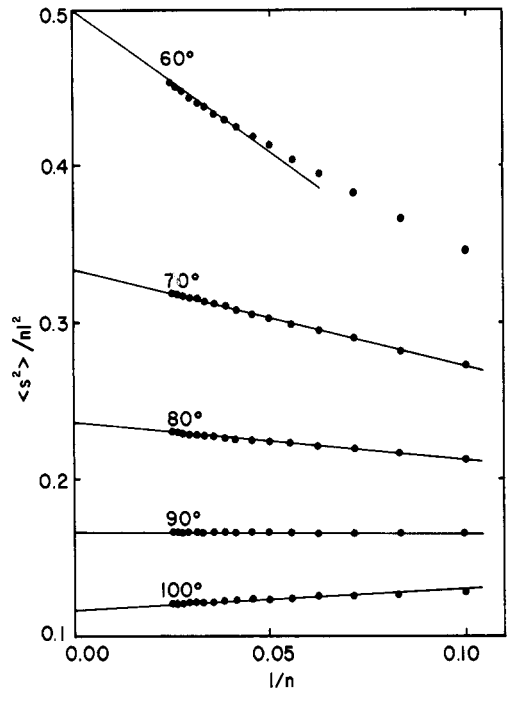

Figure 1. Characteristic ratios vs. n^{-1} for linear chains with the indicated bond angle supplements. Intercepts are the values expected from theory. Symbols plotted are always as large or larger than ± one standard deviation.

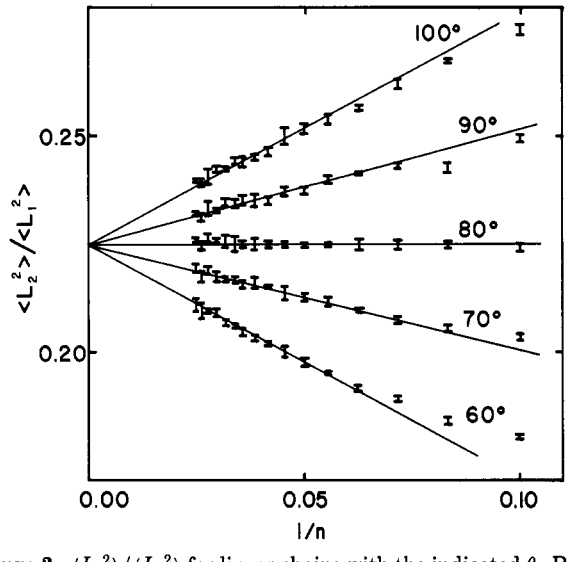

Figure 2. $\langle L_2^2\rangle/\langle L_1^2\rangle$ for linear chains with the indicated θ. Bars denote ± one standard deviation.

slopes differing by about 10% from those given by eq 2 and 3. Limiting asymmetries are clearly in harmony with those obtained in earlier Monte-Carlo calculations for linear chains. Small differences in the results reported arise from uncertainties in extrapolation and finite sample size.

Even short chains have asymmetries close to that obtained at the asymptotic limit if θ is near 80°. An increase in θ above 80° causes short chains to be less asymmetric than infinitely long chains. The converse holds if θ falls below 80°. Many polymers have θ near 70°, in which case asymmetry would be expected to decrease as n increases. This expectation is confirmed in calculated asymmetries reported for unperturbed poly(methylene),[1] poly(oxyethylene),[8] and poly(thiaethylene).[9]

Three-Stars. Figure 4 depicts behavior of characteristic ratios for molecules consisting of three chains emanating

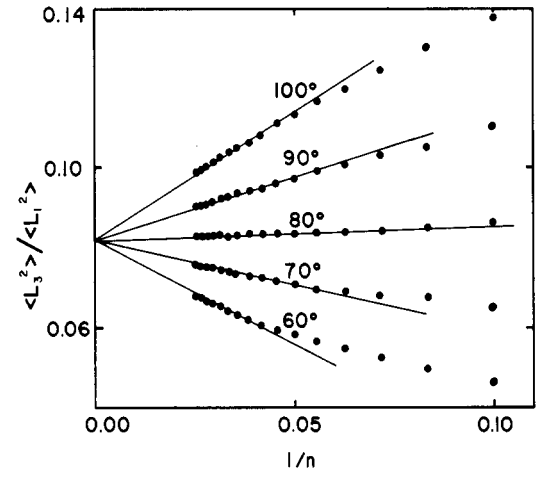

Figure 3. $\langle L_3^2\rangle/\langle L_1^2\rangle$ for linear chains with the indicated θ. Symbols plotted are larger than ± one standard deviation.

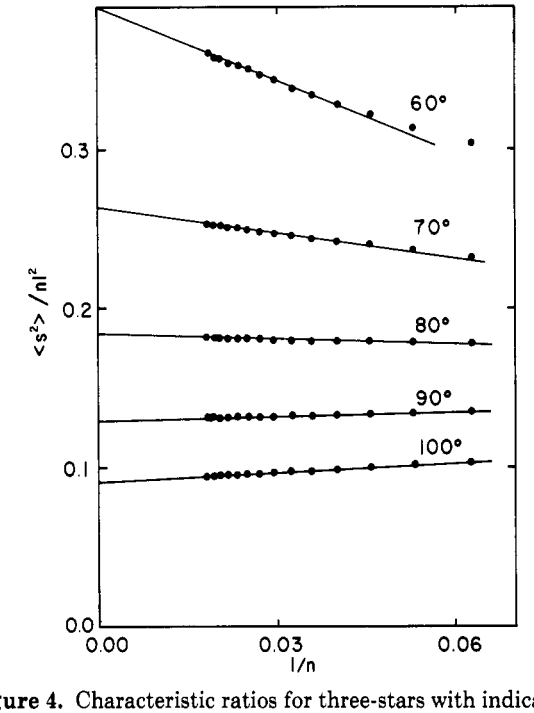

Figure 4. Characteristic ratios for three-stars with indicated θ. Each branch contains the same number of bonds. Symbols plotted are as large or larger than ± one standard deviation.

from a trifunctional branch point. Intercepts are those given by

$$[\langle s^2\rangle/nl^2]_\infty = g(1/6)(1 + \cos\theta)(1 - \cos\theta)^{-1} \quad (4)$$

where g is equal to $^7/_9$. This value for g was originally obtained with the use of random flight statistics.[14] Rotational isomeric state theory also yields this value if the branches contain a sufficiently large number of bonds.[15] Expected intercepts represent reasonable extrapolations of data for each θ.

Ratios of averaged principal components are depicted in Figures 5 and 6. Limiting values, 0.326 for $\langle L_2^2\rangle/\langle L_1^2\rangle$ and 0.116 for $\langle L_3^2\rangle/\langle L_1^2\rangle$, are in good agreement with those obtained previously with the use of a cubic lattice.[12] These limiting ratios are in each case closer to unity than those obtained with the linear chains, as expected.[12] A change from linear chain to three-star increases the limiting $\langle L_2^2\rangle/\langle L_1^2\rangle$ by 45%, while $\langle L_3^2\rangle/\langle L_1^2\rangle$ rises it by 41%.

Values of $\langle L_2^2\rangle/\langle L_1^2\rangle$ of three-stars for which computations were actually performed are slightly higher than those obtained in the limit as n approaches infinity. This

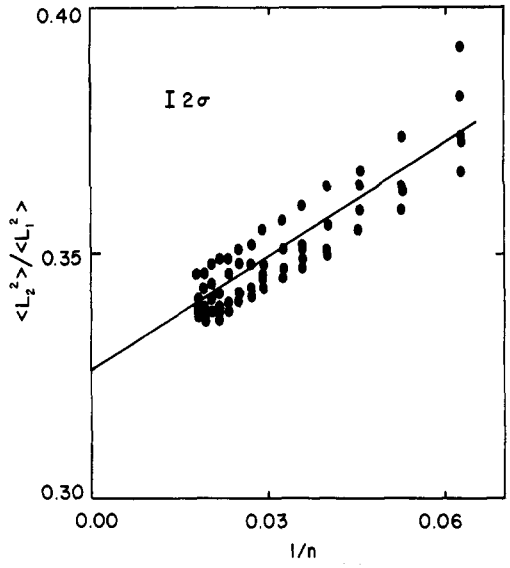

Figure 5. $\langle L_2^2\rangle/\langle L_1^2\rangle$ for three-stars with bond angle supplements of 60, 70, 80, 90, or 100°. At a particular n the larger $\langle L_2^2\rangle/\langle L_1^2\rangle$ are obtained with the larger bond angle supplements. A typical ± one standard deviation is noted; σ is roughly independent of n and θ.

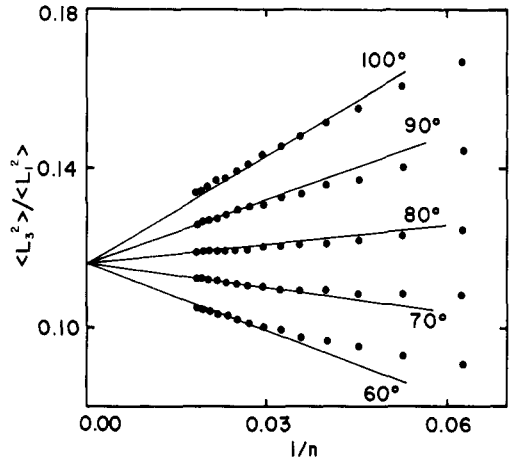

Figure 6. $\langle L_3^2\rangle/\langle L_1^2\rangle$ for three-stars with indicated θ. Symbols plotted are larger than ± one standard deviation.

situation is in contrast to that seen with linear chains, where $\langle L_2^2\rangle/\langle L_1^2\rangle$ at small n was lower than that obtained at infinite chain length if θ was less than about 80°. The general behavior of $\langle L_3^2\rangle/\langle L_1^2\rangle$ for three-stars at small n, on the other hand, is reminiscent of that seen with linear chains. Straight lines in Figure 6 are given by

$$\langle L_3^2\rangle/\langle L_1^2\rangle = 0.116 + (-2.756 + 0.0366\theta)n^{-1} \quad (5)$$

If the three-star has θ greater than about 75°, its asymmetry will increase as n increases. A more complicated situation exists if θ is less than 75°, for then $\langle L_2^2\rangle/\langle L_1^2\rangle$ decreases, but $\langle L_3^2\rangle/\langle L_1^2\rangle$ increases as n approaches infinity.

Even though unperturbed triglycerides are much more complicated than the three-stars considered here, they still exhibit behavior in accord with conclusions reached above. Thus $\langle L_2^2\rangle/\langle L_1^2\rangle$ decreases as the number of carbon atoms in the acyl substituents increases. It attains a limiting value of about $^1/_3$.[16] In contrast, $\langle L_3^2\rangle/\langle L_1^2\rangle$ increases slowly as the fatty acid substituents proceed from acetyl to stearyl. This is the result expected from Figure 6 if the effective θ for triglycerides is close to the 68° appropriate for a poly(methylene) chain.[1] The asymptotic limit for

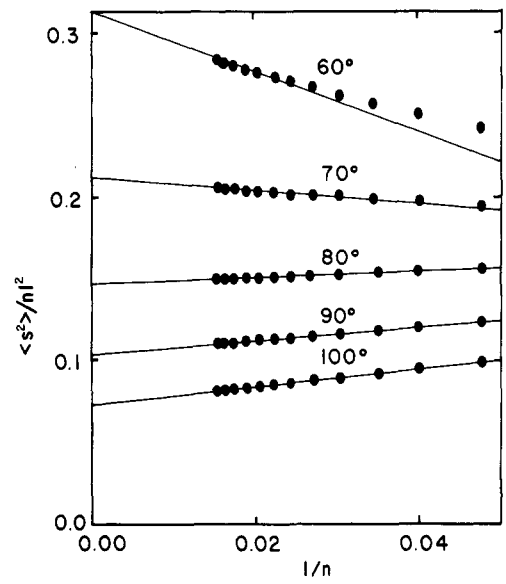

Figure 7. Characteristic ratios for four-stars with indicated θ. Each branch contains the same number of bonds. Symbols plotted are larger than ± one standard deviation.

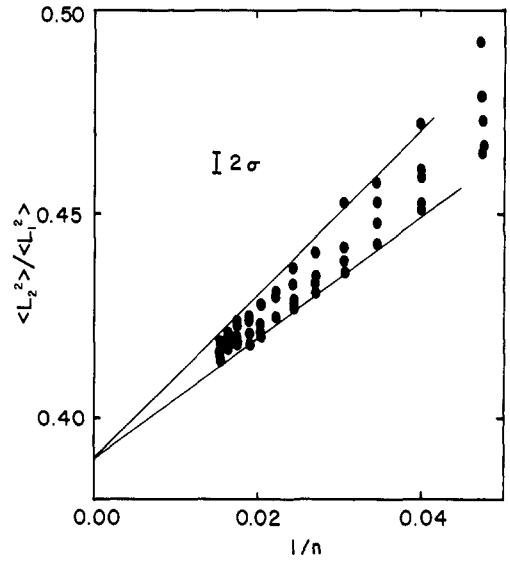

Figure 8. $\langle L_2^2\rangle/\langle L_1^2\rangle$ for four-stars with bond angle supplements of 60, 70, 80, 90, or 100°. At a particular n the larger $\langle L_2^2\rangle/\langle L_1^2\rangle$ are obtained with θ = 60°. A typical ± one standard deviation is noted; σ is roughly independent of n and θ.

$\langle L_3^2\rangle/\langle L_1^2\rangle$ is not attained by triglycerides of physiologically interesting size. The ratio of $\langle L_3^2\rangle$ to $\langle L_1^2\rangle$ is about $^1/_{12}$ for unperturbed tripalmitin, tristearin, and triolein.[16]

Four-Stars. Characteristic ratios for molecules consisting of four chains emanating from a common atom are depicted in Figure 7. Intercepts are those specified by eq 4 with $g = {}^5/_8$, in accord with random flight statistics[14] and the limiting behavior obtained with the use of rotational isomeric state theory.[15] In each case the expected intercept represents a reasonable extrapolation of the data.

Figures 8 and 9 present ratios of averaged principal components of the mean square radius. Limiting values are 0.390 and 0.153, which in each case are closer to unity than results obtained with linear chains or three-stars, as expected. Calculations performed on a cubic lattice yield ratios higher by about 5%. The change from linear chain to four-star increases the limiting $\langle L_2^2\rangle/\langle L_1^2\rangle$ by 72% and $\langle L_3^2\rangle/\langle L_1^2\rangle$ by 88%.

As was the case with three-stars (but not linear chains), $\langle L_2^2\rangle/\langle L_1^2\rangle$ at all θ used decreases as n increases through

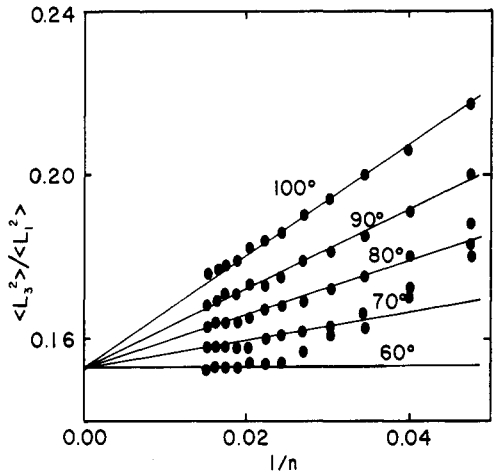

Figure 9. $\langle L_3^2\rangle/\langle L_1^2\rangle$ for four-stars with indicated θ. Symbols plotted are the size of a typical ± one standard deviation.

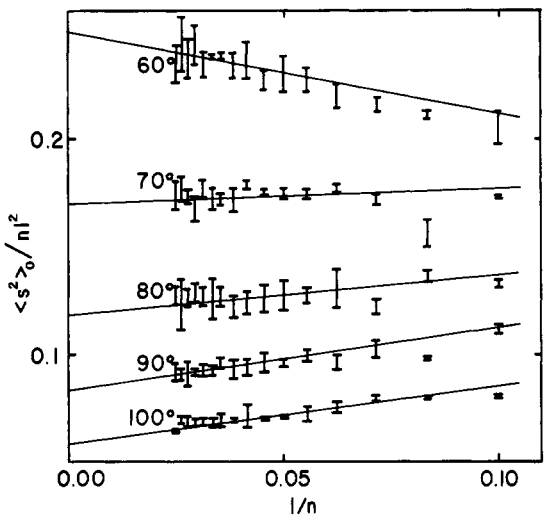

Figure 10. Characteristic ratios for macrocycles with indicated θ.

the range for which computations were executed. In contrast to *both* linear chains and three-stars, at all θ used $\langle L_3^2\rangle/\langle L_1^2\rangle$ decreases as n increases. Four of the five straight lines in Figure 9 are drawn according to

$$\langle L_3^2\rangle/\langle L_1^2\rangle = 0.153 + (-1.883 + 0.0317\theta)n^{-1} \quad (6)$$

The line for $\theta = 100°$ has a slope 6% higher than that predicted by eq 6. Asymmetry of four-stars with all θ considered becomes more pronounced as n increases. This behavior is expected because the four-star with four identical bonds and a tetrahedral branch point has $L_1^2 = L_2^2 = L_3^2$.

Macrocycles. Data for macrocycles are depicted in Figures 10–12. Standard deviations are much larger than those obtained with linear chains, three-stars, and four-stars because of the much smaller sample size (see Calculations). Characteristic ratios are depicted in Figure 10. Straight lines have intercepts given by eq 4 with $g = {}^1/_2$.[17] In each case this intercept represents a reasonable extrapolation of the data.

Figure 11 depicts $\langle L_2^2\rangle/\langle L_1^2\rangle$ at the five θ used. Straight lines are drawn according to the equation

$$\langle L_2^2\rangle/\langle L_1^2\rangle = 0.37 + (-2.18 + 0.0348\theta)n^{-1} \quad (7)$$

Consequently the slope is negative if θ is less than about 63°. The θ at which the slope is zero might differ somewhat from 63° because of the uncertainty in the data points arising from the small sample size. Nevertheless, macrocycles having tetrahedral bond angles quickly attain a value of $\langle L_2^2\rangle/\langle L_1^2\rangle$ which is essentially that found at the limit as n goes to infinity.

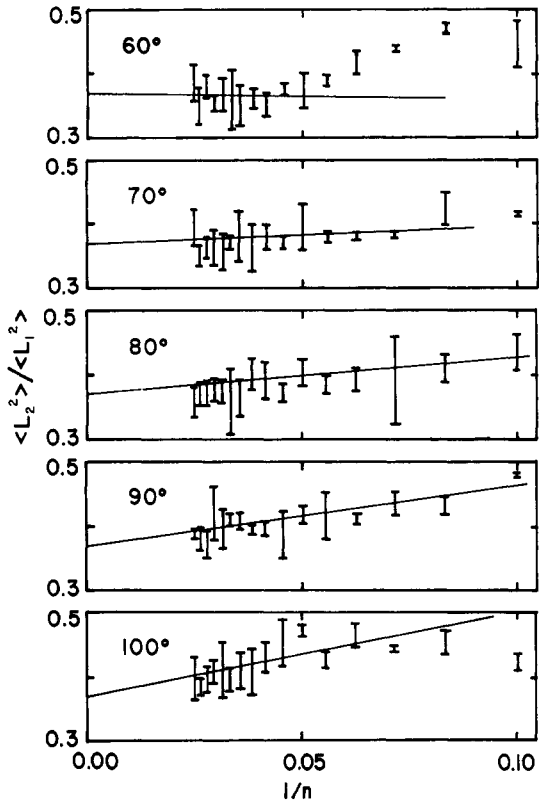

Figure 11. $\langle L_2^2\rangle/\langle L_1^2\rangle$ for macrocycles with indicated θ.

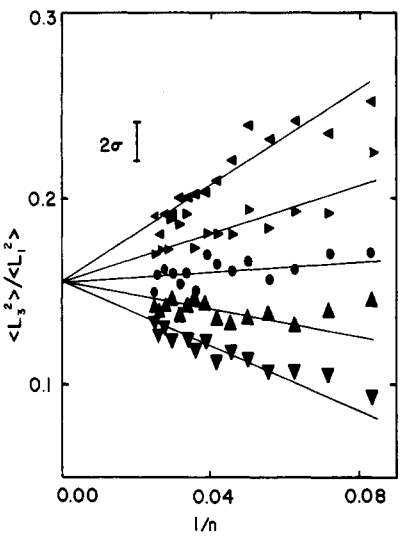

Figure 12. $\langle L_3^2\rangle/\langle L_1^2\rangle$ for macrocycles with the following θ: (▼) 60°; (▲) 70°; (●) 80°; (▲) 90°; (▼) 100°. A typical ± one standard deviation is noted; σ is roughly independent of n and θ.

The behavior of $\langle L_3^2\rangle/\langle L_1^2\rangle$ at small n is reminiscent of that seen with linear chains and three-stars (but not four-stars). Lines in Figure 12 have a positive slope if θ is greater than 77°. They are drawn according to

$$\langle L_3^2\rangle/\langle L_1^2\rangle = 0.155 + (-3.91 + 0.0507\theta)n^{-1} \quad (8)$$

Macrocycles with tetrahedral bond angles show an increase in $\langle L_3^2\rangle/\langle L_1^2\rangle$ as n increases. This behavior is exhibited in calculated asymmetries of macrocycles formed from

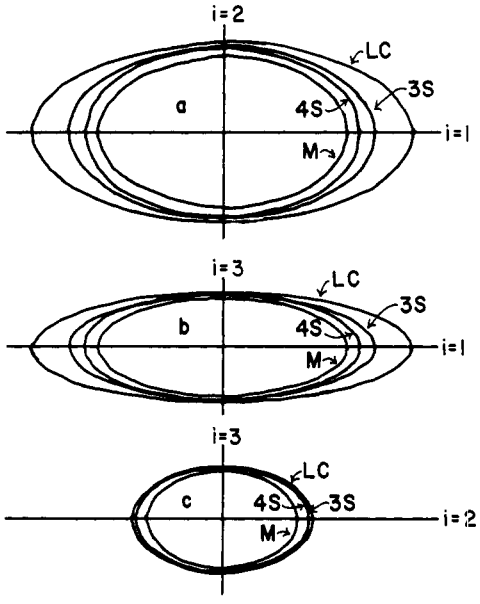

Figure 13. Ellipses whose axes are scaled according to $[\langle L_i^2\rangle/\langle s^2\rangle_{1c}]^{1/2}$. The horizontal line in each case has a length of 2 on this scale. The values for i are 1 and 2 in (a), 1 and 3 in (b), and 2 and 3 in (c). Symbols are LC for linear chain, 3S for three-star, 4S for four-star, and M for macrocycle.

poly(oxyethylene)[8] and poly(thiaethylene).[9]

Excellent agreement is obtained between the limiting asymmetries reported here for macrocycles and those obtained previously on a cubic lattice.[12] Limiting values of $\langle L_2^2\rangle/\langle L_1^2\rangle$ and $\langle L_3^2\rangle/\langle L_1^2\rangle$ are nearly identical for four-stars and macrocycles. Hence the asymmetry of a large flexible macrocycle is not easily distinguished from that of a large flexible four-star.

Averaged Principal Components of the Mean Square Radius. The above discussion of asymmetries focused attention on ratios of averaged principal moments for a given bonding pattern. Now attention is directed to the manner in which $\langle L_i^2\rangle$ for each i varies for linear chains, three- and four-stars, and macrocycles. Differences arise because alterations in asymmetry and characteristic ratio each affect $\langle L_i^2\rangle$. Discussion will be confined to the case where n is large enough to justify use of the limiting results. The necessary information is therefore obtained by dividing all $\langle s^2\rangle$ and $\langle L_i^2\rangle$ by $\langle s^2\rangle_{1c}$, the mean square unperturbed radius of gyration of the linear chain having the same θ and number of bonds. Numerical results are collected in Table III. A pictorial representation is presented in Figure 13. Here are drawn ellipses whose axes are scaled according to the $[\langle L_i^2\rangle/\langle s^2\rangle_{1c}]^{1/2}$. The view is along the axis whose principal component is L_3^2, L_2^2, and L_1^2 in Figure 13a,b,c, respectively.

The principal component most affected is seen to be the largest. Its average value increases in the order macrocycles < four-stars < three-stars < linear chains. A change from linear chain to either of the stars produces such a small effect on $\langle L_2^2\rangle$ and $\langle L_3^2\rangle$ as to be barely perceptible on the scale used in Figure 13c. Macrocycles have slightly smaller values for these two averaged principal components of the mean square radius. Nevertheless, it is still a useful approximation to view cyclization of a long linear chain as demanding a major reduction in $\langle L_1^2\rangle$ and only minor adjustment of $\langle L_2^2\rangle$ and $\langle L_3^2\rangle$. This behavior has been noted with poly(oxyethylene)[8] and poly(thiaethylene).[9]

Table III
Relative Sizes of Averaged Principal Components of the Mean Square Radius for Large Flexible Unperturbed Linear Chains, Macrocycles, Three-Stars, and Four-Stars[a]

molecule	$\langle L_1^2\rangle/\langle s^2\rangle_{1c}$	$\langle L_2^2\rangle/\langle s^2\rangle_{1c}$	$\langle L_3^2\rangle/\langle s^2\rangle_{1c}$	$\langle s^2\rangle/\langle s^2\rangle_{1c}$
linear	0.765	0.172	0.0627	1
three-star	0.495	0.162	0.0575	7/9
four-star	0.405	0.158	0.0620	5/8
macrocycle	0.328	0.121	0.0508	1/2

[a] $\langle s^2\rangle_{1c}$ denotes the mean square unperturbed radius of gyration for a long linear chain containing the same number of bonds.

The foregoing discussion suggests a physical property determined by the instantaneous distribution of atoms along the major principal axis will be more sensitive to change from linear chain to macrocycle or a three- and four-star than predicted by the effect on $\langle s^2\rangle$. On the other hand, a physical property determined by the instantaneous distribution perpendicular to this axis will be nearly identical for these four types of molecules.

Acknowledgment. Supported by NSF research Grant No. PCM 78-22916.

References and Notes

(1) D. Y. Yoon and P. J. Flory, *J. Chem. Phys.*, **61**, 5366 (1974).
(2) W. L. Mattice, *Macromolecules*, **10**, 1182 (1977).
(3) W. L. Mattice, *Macromolecules*, **10**, 1177 (1977).
(4) K. Solc and W. H. Stockmayer, *J. Chem. Phys.*, **54**, 2756 (1971).
(5) K. Solc, *J. Chem. Phys.*, **55**, 355 (1971).
(6) D. E. Kranbuehl and P. H. Verdier, *J. Chem. Phys.*, **67**, 361 (1977).
(7) W. Kuhn, *Kolloid Z.*, **68**, 2, (1934).
(8) W. L. Mattice, *Macromolecules*, **12**, 944 (1979).
(9) W. L. Mattice, *J. Am. Chem. Soc.*, **102**, 2242 (1980).
(10) M. Doi and H. Nakajima, *Chem. Phys.*, **6**, 124 (1974).
(11) T. Minato and A. Hatano, *Macromolecules*, **11**, 195 (1978).
(12) K. Solc, *Macromolecules*, **6**, 378 (1978).
(13) H. Benoit and P. M. Doty, *J. Phys. Chem.*, **57**, 958 (1953).
(14) B. H. Zimm and W. H. Stockmayer, *J. Chem. Phys.*, **17**, 1301 (1949).
(15) W. L. Mattice and D. K. Carpenter, *Macromolecules*, **9**, 53 (1976).
(16) W. L. Mattice, *J. Am. Chem. Soc.*, **101**, 732 (1979).
(17) H. A. Kramers, *J. Chem. Phys.*, **14**, 415 (1946).